ELSEVIER

Nuclear Physics B (Proc. Suppl.) 78 (1999) 663–669

NUCLEAR PHYSICS B
PROCEEDINGS
SUPPLEMENTS

www.elsevier.nl/locate/npe

Characterization of neutron irradiated Silicon Microstrip Detectors

M. Lenzi[a], E. Catacchini[a], C. Civinini[a], R. D'Alessandro[a], M. Meschini[a]

[a]Università di Firenze and INFN-Firenze, Firenze, Italy

The radiation hardness of silicon microstrip detectors has been investigated on full-size prototypes similar to the ones that will be installed in the forward tracker of CMS, where a very intense radiation environment is envisaged. Silicon detectors were exposed to a neutron beam with 3 different fluences up to 2.4×10^{14} neutrons/cm^2, more than those foreseen at LHC after 10 years of operation. Degradation effects of the device properties regarding reverse current, depletion voltage, bulk and interstrip capacitance has been measured in laboratory as function of bias voltage, temperature and neutron fluence.

1. Introduction

Future high energy experiments at LHC [1–3] will make a large use of silicon microstrip detectors for precision tracking purposes. Due to the high collider luminosity, these detectors will operate in a high radiation environment caused both by particles produced in the primary proton-proton interaction and by albedo neutrons emitted from the calorimeters surrounding the silicon tracker. Hence the need to study radiation effects on our sensors in order to be able to choose the design parameters that maximize the detector lifetime while keeping optimal performances. The macroscopic effects of radiation damage are observed with laboratory measurements of the leakage current, the full depletion voltage and the detector electrical parameters like interstrip and bulk capacitance, bias resistance, etc. Moreover, it is fundamental to check these parameters after irradiation because they greatly affect detector performances such as charge collection and noise components.

All these considerations have led us to irradiate 3 identical detectors with different neutron fluences. For the CMS silicon tracker a neutron fluence of 1.6×10^{14} neutrons/cm^2 after 10 years of operation is foreseen [4] but a safety factor of 1.5 has been considered in our test because of the uncertainties in fluence calculation and damage constants. Thus, we have irradiated our detectors with fluences up to 2.4×10^{14} neutrons/cm^2. The silicon sensors involved in the test have been characterized in laboratory before and after the irradiation.

2. Detector description

The detectors under study are single sided, full size prototypes similar to the ones that will be installed in the forward part of the CMS silicon tracker and have been manufactured by CSEM, Switzerland. The sensors follow a wedge geometry and are processed from 4 inch n-type wafers, 300 μm thick, with a resistivity of 4KΩ·cm. Each module is composed of 2 different detectors, named F1 and F2, whose strips are daisy-chained together for a detector total length of around 11.5 cm. The modules have 1024 p^+ strips with a pitch that varies from 50 μm on the narrower side to 70 μm on the wider one. The width of the strip varies with the pitch so as to have a constant width over pitch ratio. The detector layout is shown in fig. 1 and the main detector parameters

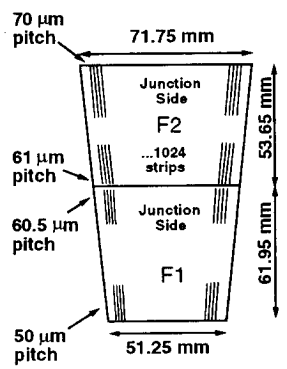

Figure 1. Detector layout.

PII S0920-5632(99)00621-0

are summerized in table 1 where N is the number of the strips, L is their average length, W their width, P the pitch and A the total active area of the detectors.

Table 1
Main detector parameters.

Det	N	L (cm)	W/P	P (μm)	A (cm^2)
F1	1024	6.21	0.28	50-60.5	35.08
F2	1024	5.37	0.23	61-70	36.02

The implant strips are AC coupled to the readout chip through integrated capacitors made with a thin insulating layer between implants and aluminium electrodes. The dielectric used in our detectors is a double layer of SiO_2 and Si_3N_4.

The choice of biasing technique must satisfy the need of high radiation resistance; in this sense the best solution is using poly-silicon resistors to connect the implants with the bias ring surrounding the sensor active area. The value of the resistors ($\sim$ 6MΩ) is a compromise between two conflicting needs; that of a low thermal noise and that of a negligible voltage drop between the strips and the bias ring, even after several years of operation when the strip leakage current will be high because of radiation damage.

3. Radiation damage to silicon detectors

Radiation effects on silicon detectors can be divided in two different classes: bulk damages and surface damages.

The first ones are due to atomic displacements in the silicon lattice induced by non-ionizing energy loss of the incident particle. The primary knock on atom and the related vacancy are very mobile in the silicon bulk; therefore they quickly recombine or form quite stable complex defects which are responsible for a change in the effective doping concentration. As an example the vacancy-phosphor complexes reduce the concentration of active donors, and the negatively charged divacancy complexes behave as acceptors. This means that increasing the irradiation fluence, the number of acceptors begins to compensate the donor population until the silicon bulk becomes intrinsic; at higher fluences, the silicon bulk inverts from n-type to p-type.

Moreover, the change of effective doping concentration leads to a change in the full depletion voltage heavily affecting the operating conditions.

Another observable effect of bulk damage is the increase of the leakage current due to the reduction of the minority carriers lifetime; this effect increases the parallel noise contribution but can be minimized by exploiting the strong dependence of current on temperature, as shown in section 6.1.

Concerning the surface damage, the most important effect is a positive charge accumulation in the oxide layer due to trapping of the holes produced by the ionizing radiation in the oxide. The main consequences of this effect are an increase in interstrip capacitance and a reduction of AC coupling capacitance. Both these effects lead to a worsening of the signal to noise ratio [5].

4. Irradiation

A set of 3 detectors were exposed to a neutron beam at 3 different fluences. Neutron irradiation was performed using the cyclotron of Institute of Nuclear Research of the Hungarian Academy of Sciences (ATOMKI), Debrecen, Hungary [6]. During irradiation the detectors were kept at room temperature and without bias voltage. After irradiation the sensors were stored at low temperature ($\sim$ -15 °C) to avoid reverse annealing effects [7]. Since the damage effects strongly depend on the neutron spectrum, to compare different sources the irradiation fluences are usually normalized to 1 MeV equivalent fluences according to ref. [8]. The 1 MeV equivalent fluences used in the present test are:

$$\phi_1 = 9.7 \times 10^{13}\ \mathrm{n/cm^2}$$
$$\phi_2 = 1.7 \times 10^{14}\ \mathrm{n/cm^2}$$
$$\phi_3 = 2.4 \times 10^{14}\ \mathrm{n/cm^2}$$

5. Experimental setup

In all our measurements, we used a Keithley 237 High Voltage Source Unit to supply the bias voltage between the bias ring on the junction side

and the back plane of the detector under test. In this configuration, the instrument allows a measurement of the total leakage current as a function of bias voltage.

For the capacitance measurement we used an HP 4284A LCR Meter that performs a measurement of a complex impedance by applying a known AC signal to the device and measuring the return current. From these values we extracted the capacitance by assuming the impedance to be the parallel between a resistance and a capacitance.

For the bulk capacitance measurement, we connected the LCR Meter between the bias ring on the junction side and the back plane of the detector. In this case a DC voltage protection network is needed to shield the inputs of the LCR Meter from bias voltage.

The interstrip capacitance was measured by connecting the LCR Meter between two adjacent metal strip and grounding the first neighbour strips; in this way their contribution is subtracted from the measurement by the instrument.

Finally, for the coupling capacitance we connected the LCR Meter between the implant and the metal of the same strip.

All the measured capacitances show a strong frequency dependence explained by the fact that the detector elements form a network of resistors and capacitors that cannot be schematized as a simple RC parallel. Each measure shown in this paper is taken at a frequency where the capacitance reaches a plateau level; for this frequency value, the impedance phase is about 90^0 thus purely capacitive.

Finally, the bias resistance measurements were performed by applying a small difference voltage across the resistance and measuring the current through that resistor. This measurement is carried out using an HP 4145B Semiconductor Parameter Analyzer.

All these measurements were performed before irradiation using a probe station at room temperature ($\sim$ 24 °C). After irradiation, to avoid high leakage current interference with the measurements, we performed most of our tests in a climatic chamber at low temperature, microbonding the metal strips to external gold pads connected to the instruments. Some measurements like that of the coupling capacitance and bias resistance (that need to contact the implant strip), had to be carried out at room temperature inside the probe station, with a worse precision. Moreover, for the same reason, it was impossible to perform these two measurements for the most irradiated detector because, at room temperature, the leakage current exceeded the voltage source current limit.

6. Experimental results

All the measurements presented in this paper regard the F1 detectors but comparable results have been found for the F2 detectors also.

6.1. Leakage current

For the whole set of detectors, we measured the leakage current as a function of bias voltage and temperature. In fig. 2 the results of the measurements at -10 °C are shown.

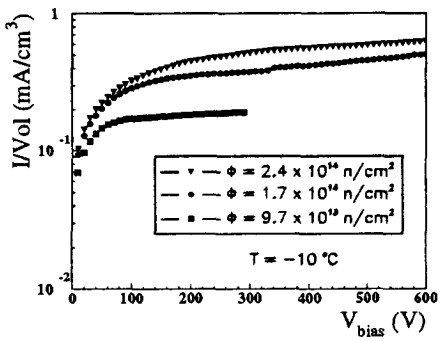

Figure 2. Leakage current for the F1 irradiated detector at -10 °C.

For each detector, we took data changing the temperature from +5 °C to -25 °C with steps of 5 °C and we fitted the measured points to the formula describing current generation in a reverse biased junction [9]:

$$I \propto T^{3/2} exp(-E_a/kT) \quad (1)$$

The results are shown in fig. 3 for the most irradiated detector.

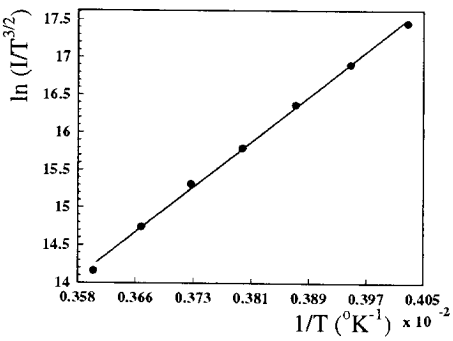

Figure 3. Temperature dependence of the leakage current for the most irradiated detector.

The average value for E_a turns out to be (0.60 ± 0.05) eV and no systematic dependence of E_a on neutron fluence has been observed.

The degradation effects on the current due to irradiation are described in terms of an increase in the current density that scales linearly with the fluence ϕ:

$$\frac{\Delta I}{Volume} = \alpha\phi \qquad (2)$$

where α is referred to as the "damage constant". In fig. 4 is shown the result for the F1 detectors at -10 °C; the obtained value for α and its temperature dependence are in agreement with other measurements in literature [10].

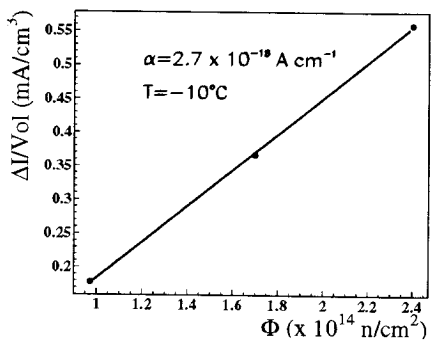

Figure 4. Measurement of the damage constant for the F1 irradiated detectors at -10 °C.

6.2. Bulk capacitance and full depletion voltage

A measurement of the bulk capacitance is fundamental to the characterization of a silicon detector; in fact its behaviour as a function of the bias voltage determines the full depletion voltage. Modeling the detector as a parallel plate capacitor, we expect that the junction capacitance decreases with the applied voltage till the depletion layer reaches the back of the detector. The capacitance then remains constant and its value coincides with the expected geometrical one. The bulk capacitance per unit area can be written as [9]:

$$C_{bulk} = \begin{cases} \sqrt{\frac{q\epsilon_{si}N_{eff}}{2V_{bias}}} & V_{bias} < V_{depl} \\ \frac{\epsilon_{si}}{d_{depl}} & V_{bias} > V_{depl} \end{cases} \qquad (3)$$

where d_{depl} is the maximum depth of the depletion layer that is the thickness of the bulk and N_{eff} is the effective doping density defined as the difference between the number of donors and acceptors. The depletion voltage is extracted from a plot of $1/C^2$ versus V_{bias} as the intersection of the plateau value after full depletion and a linear fit at lower voltage, as shown in fig. 5.

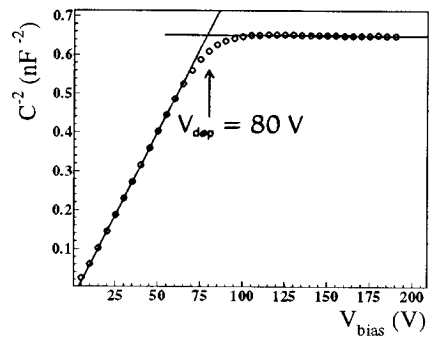

Figure 5. Extrapolation of the full depletion voltage for the non irradiated detector.

In fig. 6 is shown the measured bulk capacitance as a function of bias voltage for irradiated and non irradiated detectors.

These measurements are performed at -25 °C to minimize the influence of the leakage current on the results. The value of the plateau is in

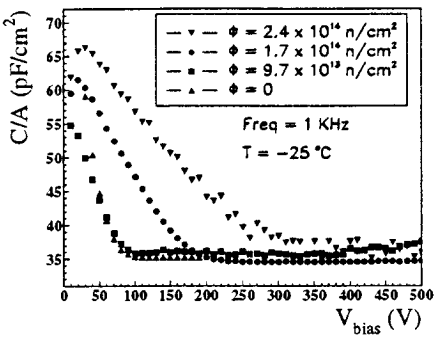

Figure 6. Measurement of the bulk capacitance for the set of F1 detectors.

good agreement, even after irradiation, with the one calculated from (3), that is 34.5 pF/cm^2 for our detectors. In table 2 the full depletion voltage for the whole set of detectors is shown.

Table 2
Full depletion voltage before and after irradiation.

ϕ ($\times 10^{14}$n/cm^2)	0	0.97	1.7	2.4
V_{depl} (V)	80	90	200	310

6.3. Effective doping concentration

Knowing the full depletion voltage, the effective doping concentration N_{eff} is obtained from [9]:

$$|N_{eff}| = \frac{2\epsilon_{si} V_{depl}}{q d_{depl}^2} \quad (4)$$

Several experimental data have been found in agreement with an empirical model [11] where the change of N_{eff} due to irradiation, in absence of annealing effects, is expected to depend on the neutron fluence as the sum of two opposite contribution: a decrease of donors, exponential with fluence, and an increase of acceptors, linear with fluence:

$$N_{eff,0} - N_{eff} = N_{C0}(1 - exp(-c\phi)) + g_c\phi \quad (5)$$

where $N_{eff,0}$ is the effective doping concentration before irradiation. N_{C0} is closely related to the initial doping concentration and can be thought of as the number of removable donors; the fact that $N_{C0} < N_{eff,0}$ means that only a part of the initial donors became electrically inactive after irradiation [12]. The quantities g_c and c are named respectively acceptor creation and donor removal parameter.

To compare our results with this model, we calculated N_{eff} from (4) and fitted the experimental data with the expected behaviour described by (5). The results are shown in fig. 7; the obtained values for the fit parameters are in agreement with other results in literature [12] and seem to confirm the model at least concerning the acceptor creation that is the dominant effect in the fluence region where our experimental points are located. The neutron fluence needed for silicon type invertion depends strongly on the initial doping concentration, hence on the bulk resistivity. For our detectors the inversion fluence turns out to be 4 $\times$ 10^{13} neutrons/cm^2; this means that, in the framework of this model, all our irradiated devices are type inverted.

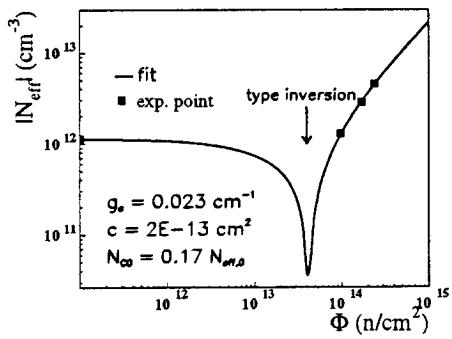

Figure 7. Effective doping concentration as function of neutron fluences.

6.4. Bias Resistance

The type inversion observed in fig. 7 is confirmed by the behaviour of the bias resistances as a function of the bias voltage shown in fig. 8 for irradiated and non irradiated detectors.

Before irradiation, the bulk is n-type and the depletion starts on the junction side; therefore the resistance is isolated from the bulk even at

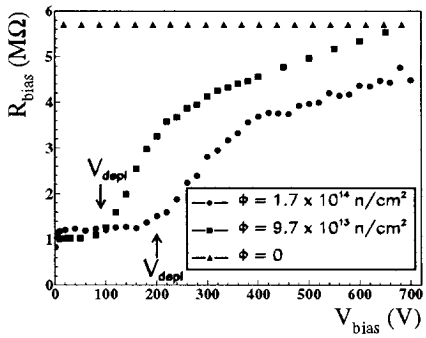

Figure 8. Measurement of the bias resistance for the set of F1 detectors.

low bias voltage and consequently it remains constant. On the contrary, after irradiation and type inversion, the depletion starts on the ohmic side; consequently the resistance starts to be isolated from the bulk only after full depletion.

6.5. Interstrip Capacitance

The capacitance between two adjacent strip is the main component of the total capacitance which the amplifier senses on its input and it should be minimized for best noise performance. The coupling of two adjacent strips is determined, not only by the silicon material between the p^+ implants, but also by the accumulation layer of free electrons at the silicon-oxide interface. This layer is induced by the positive charges, always present in the oxide, and act as a thin conductor, thus increasing the capacitance. Before irradiation, two adjacent strips are isolated even at very low voltage and we observe only a slow decrease of the capacitance with voltage due to the increase of the width of the depleted gap between the p^+ strip and the electron layer [13]. After irradiation, the concentration of positive fixed charge in the oxide and consequently the negative charge at the interface are higher. These changes make the interstrip coupling higher than before irradiation. When the depletion reaches the strip side, the capacitance decrease sharply by increasing the bias voltage up to a value two times higher than the one at full depletion. After that it continues to decrease slowly due to the further confinement of the electron charge, in the same way as for non irradiated detectors. Fig. 9 shows this capacitance for the whole set of detectors as a function of bias voltage.

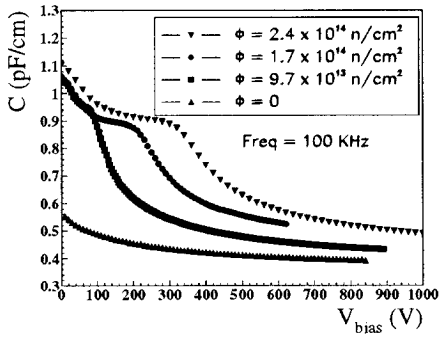

Figure 9. Measurement of the inter-strip capacitance for the set of F1 detectors.

The measurement plotted in figure are taken at T=-10 °C but we verified that there is no significant change in capacitance with temperature.

6.6. Coupling Capacitance

The coupling capacitance couples the charge produced by an ionizing particle and collected in the implant strip to the read-out aluminium strip. As explained in section 3, the irradiation produce a positive charge accumulation in the oxide layer that decrease the value of the coupling capacitance. The results of this measurement are shown in fig. 10.

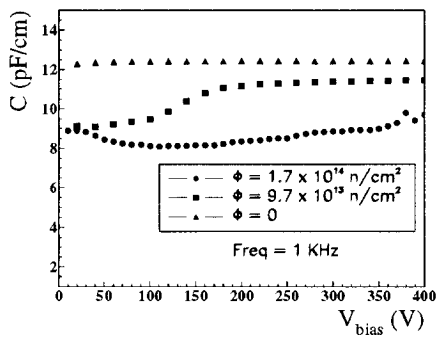

Figure 10. Measurement of the coupling capacitance for the set of F1 detectors.

This reduction slightly affects the charge collection mechanism increasing the fraction of signal that is transferred to the detector backplane and consequently lost.

7. Conclusions

Radiation damage, both regarding bulk and surface effects, have been investigated on 3 silicon detectors irradiated with different neutron fluences up to 2.4×10^{14} neutrons/cm^2.

The obtained results may be summerized as follows:

- The dependence of the effective doping concentration on neutron fluences is well described by a simple model that provides an exponential donor reduction and a linear acceptor creation with fluence. The free parameters of this model have been extracted from our data. In particular, the inversion fluence for our detectors has been found to be 4×10^{13} neutrons/cm^2; hence all our irradiated detectors have undergone bulk inversion from n-type to p-type.
- Strictly connected to the change of effective doping concentration is the change of the full depletion voltage that increases up to 310 V for the most irradiated detector.
- Due to bulk damage, the leakage current increase after irradiation linearly with fluence and the extracted damage constant turns out to be 2.7×10^{-18} A/cm at T = -10 °C. However, even after irradiation, the leakage current continues to follow the expected dependence on temperature.
- The main surface effects are an increase of the interstrip capacitance that produces a worsening of the serial noise and a decrease of the coupling capacitance that reduces the charge collection efficiency.

The collected results indicate that the use of silicon detectors seems possible up to the foreseen fluence for 10 years of LHC operation. In particular, the full depletion voltage remain acceptable for irradiated prototypes. Moreover, our data show that some expedient are needed to improve the detector performances: low temperature to reduce the parallel noise due to the leakage current and over depletion of the detectors to reduce the surface effects that degrade the signal to noise ratio.

Acknowledgments

We wish to thank the staff of the irradiation facility at the Institute of Nuclear Research of the Hungarian Academy of Sciences (ATOMKI), Debrecen, Hungary and in particular J. Molnar and A. Fenyvesi for their support during irradiation.

REFERENCES

1. LHC: The Large Hadronic Collider Conceptual Design, CERN/AC/95-05 (LHC, october 1995).
2. CMS, Technical Proposal, CERN/LHCC 94-38 LHCC/P1, 15 December 1994.
3. ATLAS, Technical Proposal, CERN/LHCC 94-43 LHCC P2, 15 December 1994.
4. The Tracker Project, Technical Design Report, CERN/LHCC 98-6 CMS TDR 5, 15 April 1998.
5. C. Bozzi, CMS Note 97-026 (1997).
6. J. Molnar et al., Nucl. Instr. and Meth. B 143 (1998) 536.
7. E. Fretwust et al., Nucl. Instr. and Meth. A 342 (1994) 119.
8. ASTM E772-96.
9. S.M. Sze, Physics of Semiconductor Devices (Wiley, New York, 1981).
10. T. Ohsugi et al., Nucl. Instr. and Meth. A 265 (1998) 105.
11. A.J. Matthews et al., Nucl. Instr. and Meth. A 381 (1996) 338.
12. H. Feick et al., Nucl. Instr. and Meth. A 377 (1996) 217.
13. A. Longoni et al., Nucl. Instr. and Meth. A 288(1990) 35.